Radiation Measurements 56 (2013) 44–48

Contents lists available at SciVerse ScienceDirect

Radiation Measurements

journal homepage: www.elsevier.com/locate/radmeas

Intrinsic and radiation-induced defect luminescence of gadolinium molybdate under UV- and VUV-excitation

I.A. Gofman [a,*], V.A. Pustovarov [a], N.I. Lobachevskaya [b], V.D. Zhuravlev [b]

[a] Ural Federal University, Mira Str. 21, 620002 Yekaterinburg, Russia
[b] Insitute of Solid State Chemistry, Ural Branch of RAS, Pervomayskaya Str. 91, 620990 Yekaterinburg, Russia

HIGHLIGHTS

- Luminescence of gadolinium molybdate was studied using synchrotron radiation.
- Efficient energy transfer from Gd^{3+} to $(MoO_4)^{2-}$ centers was observed.
- New luminescent center was registered after irradiation of crystals with fast electrons.
- Variation of crystal structure led to the changes in luminescent properties.

ARTICLE INFO

Article history:
Received 15 October 2012
Received in revised form
21 January 2013
Accepted 25 January 2013

Keywords:
Gadolinium molybdate
Energy transfer
Radiation-induced defects
Intrinsic luminescence

ABSTRACT

A study of intrinsic luminescent properties of two polymorphic modifications of gadolinium molybdate was conducted using synchrotron radiation at low temperature. Excitation spectra in the UV- and VUV-ranges ($E_{exc} = 3.7–21$ eV) were measured. Energy transfer from Gd^{3+} to $(MoO_4)^{2-}$ centers was observed. Change of crystal structure influenced luminescent properties, with less symmetric phase having higher quenching temperature and lower emission. After irradiation of the crystals with fast electrons, the creation of a new luminescent center was registered with a separate excitation and emission bands. Temperature dependences of luminescence yield of all bands were measured.

1. Introduction

Gadolinium molybdate $Gd_2(MoO_4)_3$ (hereafter referred to as GMO) is well known as one of the first ferroelectric–ferroelastic crystals (Zeidler and Ullman, 1973), however in the last decade several papers were published devoted to luminescence of GMO doped with rare earth ions (Guo et al., 2008; He et al., 2010; Pan et al., 2007). In spite of this, intrinsic luminescent properties of GMO were never studied in detail, though it is of particular interest because of the presence of Gd^{3+} ions as cations in the matrix.

Recently luminescent properties of other molybdates also attracted attention of researchers, which is caused both by problems in understanding of the dynamics of electronic excitations in this type of compounds as well as their potential application as phosphors for LEDs. Most research has been carried on molybdates crystallizing in scheelite structural type (space group $I4_1/a$), including calcium, strontium, barium, lead and cadmium molybdates. Investigations of their luminescent properties using synchrotron radiation are presented in the literature (Mikhailik et al., 2005; Spassky et al., 2005).

GMO crystal structure differs from scheelite, being less symmetric; therefore it seemed interesting to compare luminescent properties between them. Two polymorphic modifications of gadolinium molybdate were studied in order to better understand the influence of symmetry and density of crystal structure on spectral properties of intrinsic luminescence in the wide range of excitation energies.

Radiation induced defects in molybdates were never an object of thorough research. Of all compounds with scheelite-like structures, only radiation hardness of lead tungstate was investigated deeply, due to its application in high energy physics. In this paper an analogy between intrinsic defect centers in molybdates and defects in electron-irradiated GMO single crystals is presented, which is both important for studying radiation hardness of molybdates as well as understanding the nature of defect molybdate centers.

* Corresponding author. Experimental Physics, Ural Federal University, Mira Str. 21, 620002 Yekaterinburg, Russia. Tel.: +7 343 375 47 11; fax: +7 343 374 43 91.
E-mail address: ilya.gofman87@gmail.com (I.A. Gofman).

1350-4487/$ – see front matter © 2013 Elsevier Ltd. All rights reserved.
http://dx.doi.org/10.1016/j.radmeas.2013.01.058

2. Crystal structure of gadolinium molybdate

Monoclinic α-phase (space group *C2/c*) is the stable polymorphic modification of GMO at room temperature. However, when growing single crystals from melt, it crystallizes in high-temperature β-form, but during even very slow cooling no phase transition to low-temperature α-form occurs because of large (about 24%) difference in unit cell volume between phases. Thus the single crystal stays in overcooled high-temperature phase at room temperature, namely in its paramagnetic (Curie temperature $T_c = 158–163°C$) orthorhombic (space group Pba2) β'-modification (Keskar et al., 2009). However during solid state synthesis procedure of GMO, the reaction temperature is insufficient for the phase transition between α- and β-forms, therefore the derived powders are in α-phase.

Fig. 1(a) depicts the crystal structure of monoclinic α-GMO. Gadolinium forms GdO_8 polyhedra which share a common edge. The shortest Gd–Gd distance is 3.91 Å. There are two inequivalent molybdate tetrahedra with average Mo–O distance of about 1.75 Å. The shortest Mo–Mo distance is 5.0 Å.

Crystal structure of orthorhombic β'-phase is shown in Fig. 1(b). Gadolinium forms GdO_7 polyhedra with shortest Gd–Gd distance of 3.91 Å. Average Mo–O distance is also 1.75 Å.

The two structures differ significantly in symmetry and unit cell volume, with almost equal sizes of molybdate anions, but more pronounced change in size of cationic position.

3. Samples and experimental details

Monoclinic α-gadolinium molybdate was synthesized by citrate technique using Gd_2O_3 (99.99%), ammonium molybdate $NH_4Mo_7O_{24}\cdot 4H_2O$ (analytic grade), citric acid, nitric acid HNO_3 (chemical grade) as initial compounds. Gadolinium oxide was dissolved in diluted nitric with constant stirring. Ammonium molybdate and citric acid preliminarily dissolved in water were added to gadolinium nitrate. The ratio between cations of metal and citric acid was 1:3. Transparent solution was produced with pH = 7–8 due to ammonium addition. Then the solution was steamed on water bath until the formation of light brown gel, which after drying was annealed in furnace at $T = 700–750°C$ during 5–10 h to produce white fluffy powder.

According to XRD data (Fig. 2) single phase composition of samples was proved along with their structural correspondence to JCPDS card 25-0338. Unit cell parameters were estimated as follows: $a = 7.5291$Å, $b = 11.4055$Å, $c = 11.4281$Å, $\beta = 109.24°$. Average grain size was estimated at 2–3 μm.

The phase composition was controlled by XRD analysis using DRON-2.0 and Shimadzu XRD-700 setups with Cu K_α radiation. Sample morphology was tested using SEM technique at JEOL JSM 6390LA setup and energy-dispersing analyzer JEOL JED 2300. SEM image of α-GMO powder is presented in Fig. 3.

Single crystals of β'-GMO were grown at Ferroelectrics Laboratory at Ural Federal University using Czochralski technique from melt in a platinum crucible in air atmosphere. In studies we used single-crystal platelets 0.7 mm thick, cut perpendicular to optical C_6axis.

A research was conducted on β'-GMO single crystals irradiated with fast electrons ($E = 10$ MeV, fluence $f = 2\cdot 10^{16}$ electron/cm^2). Sample irradiation was accomplished at M-20 microtron at Experimental Physics Department in Ural Federal University.

Absorption spectra were measured at room temperature using Helios Alpha spectrophotometer. Temperature dependences of photoluminescence (PL) yield were studied in 90–300 K temperature range with the setup including a 400 W deuterium discharge lamp with the continuous UV emission spectrum, DMR-4 double prismatic monochromators, and FEU-106 photomultiplier as light detector.

PL spectra, PL excitation spectra were measured by means of low-temperature VUV spectroscopy method at the SUPERLUMI station (HASYLAB, DESY, Hamburg) using synchrotron radiation. The 2 m vacuum monochromator with interchangeable gratings covered with Al (spectral resolution 3.2 Å) was used to excite PL in 3.7–21 eV range. The 0.3 m ARC Spectra Pro-300i monochromator, equipped with either R6358P (Hamamatsu) photomultiplier was used as a registration system. Sodium salicylate was applied to normalize PL excitation spectra to the same photon number irradiating the sample.

4. Results and discussion

4.1. Intrinsic luminescence under excitation in UV–VUV range

Intrinsic luminescence of molybdates is commonly attributed to radiative decay of self-trapped excitons (STE) localized at $(MoO_4)^{2-}$ ions (Itoh, 2012). It is typically presented with broad emission band with maximum in the green or orange spectral area. Both α- and β'-phases of gadolinium molybdate exhibit this type of emission at low temperatures. PL spectra of α- and β'-GMO are shown in Fig. 4 (curves 1, 2). They appear as wide bands with maxima $E_{emis} = 2.2$ eV (FWHM = 0.54 eV) and $E_{emis} = 2.4$ eV (FWHM = 0.63 eV), respectively.

PL excitation spectra are shown in Fig. 5 (curves 1, 2). The main excitation peak is situated near $E_{exc} = 4.5$ eV in all studied samples,

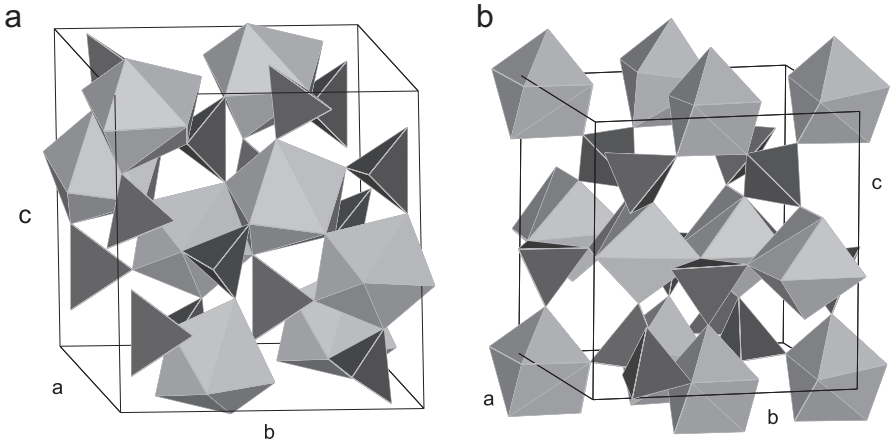

Fig. 1. Crystal structure of α-GMO (a) and β'-GMO (b) visualized using VESTA software (Momma and Izumi, 2011).

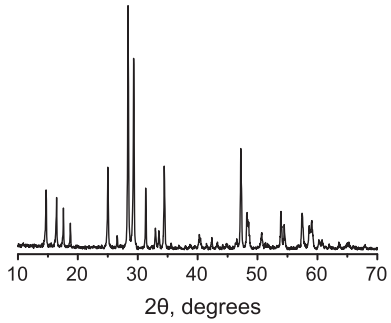

Fig. 2. Diffraction pattern of α-GMO samples.

there is also a second excitation peak near E_{exc} = 6.0 eV. As the emission was ascribed to the STE, position of the first peak can also be regarded as a rough estimate of the band gap E_g, which generally agrees with the values obtained by theoretical calculations for other molybdates (Zhang et al., 1998).

Sharp peaks near E_{exc} = 3.97 eV were attributed to $^8S_{7/2} \rightarrow {}^6P_J$ transitions in Gd^{3+} ion contained in the lattice. Peaks at this energy are also clearly seen at the absorption edge of β′-GMO (Fig. 6) of both pure and irradiated crystals. In the α-phase this peak was not observed. We were able to resolve separate peaks of Gd^{3+} absorption in this region of excitation spectra at T = 8 K (see Fig. 5, inset).

The appearance of gadolinium absorption peaks in the excitation spectra means that there exists an efficient energy transfer mechanism from cationic sublattice to the main luminescent center – molybdate tetrahedra. There is a spectral overlap between Gd^{3+} and $(MoO_4)^{2-}$ ions, while the latter has large oscillator strength, because the charge transfer transitions are direct and allowed. Therefore, the energy transfer can be of resonant type, effective, and with large critical distance (Blasse and Grabmaier, 1994). It is not clear why this energy transfer was not observed in α-GMO. Increase in the possibility of the energy migration via Gd sublattice could explain it, but it is unlikely, because the shortest Gd–Gd distance remains the same – about 3.9 Å.

4.2. Radiation-induced defects

Irradiation of β′-GMO single crystals with fast electrons produced slight yellow coloration, which is related to the red shift of absorption edge of the crystals. At room temperature the shift of the Urbach tail is estimated at 0.08 eV. Absorption spectra of the crystals before and after e-beam irradiation are presented in Fig. 6.

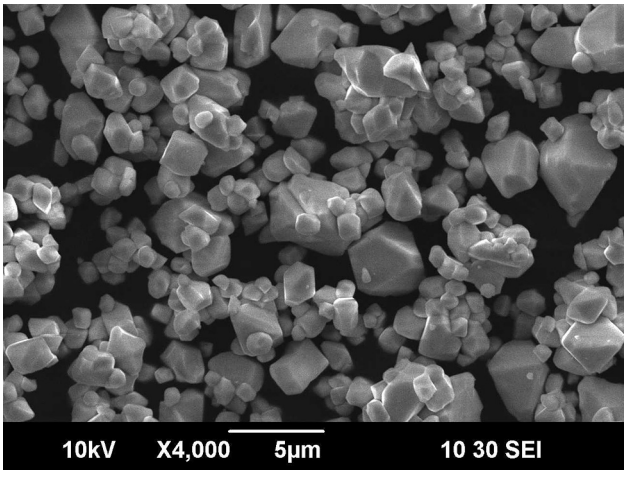

Fig. 3. SEM image of α-GMO powder.

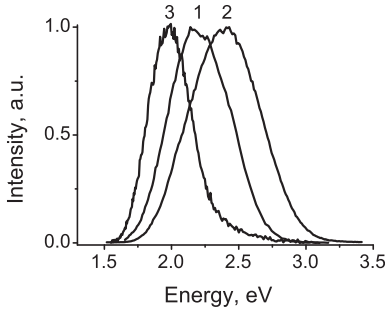

Fig. 4. Emission spectra at T = 8 K: α-GMO, E_{exc} = 4.6 eV (1); β`-GMO, E_{exc} = 4.6 eV (2); irradiated β′-GMO, E_{exc} = 3.92 eV (3).

Intrinsic emission in irradiated crystals was quenched, however a new PL band was observed. Its PL spectra peaked at E_{emis} = 1.98 eV, while its main selective excitation peak was situated near E_{exc} = 4.03 eV at T = 8 K with a weak impact from Gd^{3+} lines. The spectra are shown in Fig. 4 (curve 3) and 5 (curve 3, inset curve 2). These bands were also observed at T = 90 K using laboratory equipment with slightly shifted spectral parameters: the maximum of selective excitation band E_{exc} = 3.92 eV and maximum of emission band E_{emis} = 1.92 eV, FWHM = 0.4 eV.

Location of the induced absorption in the absorption edge region shows that defect centers are situated in the anion sublattice, because $(MoO_4)^{2-}$ groups are responsible for the formation of the band gap. As the energy of used electron beam was high (E_e = 10 MeV), the main mechanism of defect creation should be the mechanism of elastic displacement. The most probable defect in this type of compound is an oxygen vacancy, and the defect emission was earlier ascribed to the emission of the self-trapped exciton, localized at the center containing a molybdate tetrahedra and this vacancy (Blasse, 1980). This leads to an effective center formula $MoO_4 + V_O = MoO_3$. This model is supported by several considerations. First of all, excitation and absorption energies are close enough to that of the defect-free MoO_4 centers. This implies that defective center forms localized levels in the band gap near the bands and absorbs energies near the edge, shifting the Urbach tail. Smaller FWHM of the defect PL emission band is probably due to the poor spectral sensitivity of the photomultiplier tube in the near infrared spectral region. Also PL emission with similar spectral parameters was observed earlier in molybdates, including GMO, even without crystal irradiation (Ouwerkerk et al., 1982). This means that in the mentioned work the concentration of intrinsic oxygen vacancies was rather high, while in our case it was smaller, which is why this emission was not observed prior to irradiation.

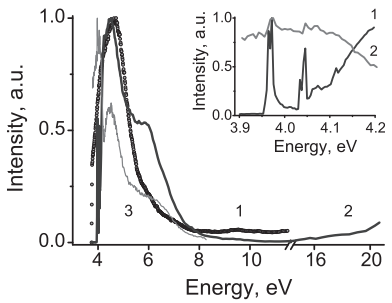

Fig. 5. Excitation spectra at T = 8 K: α-GMO. E_{emis} = 2.48 eV (1); β′-GMO, E_{emis} = 2.58 eV (2); irradiated β′-GMO, E_{emis} = 1.97 eV (3). Inset: fragments of β′-GMO (1) and irradiated β′-GMO (2) excitation spectra in the region of Gd^{3+} absorption lines.

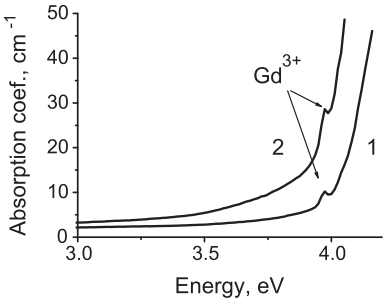

Fig. 6. Absorption spectra of pure (1) and irradiated (2) β'-GMO crystals at $T = 300$ K.

Another type of defects, which could be formed upon fast electron irradiation, is F- or F^+- center. However, existing calculations of the energy structure of these types of centers in molybdates (Guo et al., 2009) show that they should induce absorption bands in the yellow and red spectral regions, which was not observed in our case, and defect center emission experienced no re-absorption in this spectral region. Unfortunately, there is yet no data available on the EPR spectroscopy of the irradiated samples, which could make the nature of the centers more clear.

Because of the overlap between the emission and excitation spectra of the two centers, both emissions can be excited by the same energy, which was also mentioned in Ouwerkerk et al. (1982). However, excitation spectra of emission in the non-overlapping spectral area, for example at $E_{emis} = 1.77$ eV, does not contain the intrinsic excitation band. This means that no energy transfer from normal to defective luminescence centers was observed.

4.3. PL temperature dependence

Temperature dependences of relative PL emission intensities are presented in Fig. 7, they differ significantly. Luminescence of α-phase is still detectable even at room temperature, while β'-GMO emission is almost completely quenched by $T = 150$ K. Quenching temperature of the emission of the centers associated with radiation-induced defects is between the two phases.

Of all three specimen, only temperature dependence of irradiated β'-GMO crystals reach the saturation at the starting temperature $T = 110$ K. It was subject to quantitative analysis using well-known Mott's formula $I(T)/I_0 = (1 + C\cdot\exp(-\Delta E/kT))^{-1}$, where $I(T)$ denotes emission intensity, I_0 – intensity at low temperature, ΔE – activation energy. The curve was well fitted with the Mott's equation; activation energy was estimated at 0.13 eV, which agrees with those estimated for other molybdates (Mikhailik et al., 2005).

Denser crystal structure of α-GMO could also trigger the thermally activated concentration quenching, because the molybdate tetrahedra, where the self-trapped excitons are localized, become closer to each other. However, no evidence of this migration was found, which points to the intra-center temperature quenching mechanism.

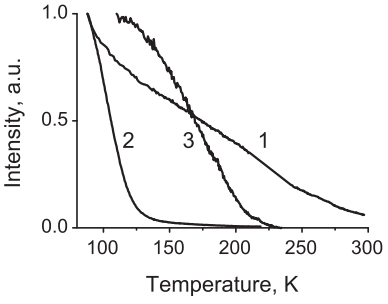

Fig. 7. Temperature dependences of relative PL intensities in α-GMO, $E_{exc} = 4.5$ eV (1), β'-GMO, $E_{exc} = 4.5$ eV (2) and irradiated β'-GMO, $E_{exc} = 3.9$ eV (3).

4.4. Influence of crystal structure on luminescent properties

Emission spectrum of α-GMO was shifted by about 0.25 eV to the lower energies compared to the β'-GMO emission spectrum. However, FWHM and corresponding excitation energies remained similar, both being in the range typical for other molybdates (Blasse, 1980). Therefore it can be ascribed to emission of the same center, influenced by the change in the crystal structure between the phases.

It was established that the emission spectrum of triplet self-trapped exciton emission in tetraoxyanions is formed by 4 interactions – Jahn-Teller, pseudo-Jahn-Teller, ligand field effects and spin–orbit interaction (Bacci et al., 2002). Lowering of the symmetry of the lattice could influence all mentioned interactions and change the profile of the emission spectrum, including the position of its maximum.

At the same time, the main excitation peak energy has equal values in both phases. It is attributed to inter-band transitions also described as the $O^{2-} \rightarrow Mo^{6+}$ charge transfer. The bonding in the MoO_4 polyhedra is significantly covalent, with bond lengths mostly decided by differences in electronegativities between Mo and O. This is why the molybdate tetrahedra have almost equal sizes in α- and β'-phases, despite the difference in density, which governs the equal transition energy and band gaps in these materials.

It was pointed out in the literature (Keller et al., 1988) that molybdates with denser structure often exhibit higher luminescence intensity, lower Stokes shift and higher quenching temperatures, because denser surroundings of molybdate tetrahedra prevent them from expansion in the excited state, which lowers the probability of non-radiative return from the excited to the ground state. However, the Stokes shift appeared higher for the denser phase, which proves that it is related to the symmetry more than density of the crystal structure.

5. Conclusions

Intrinsic luminescence in gadolinium molybdate was investigated in the wide range of excitation energies. Spectral and temperature quenching parameters of the main luminescent center were measured.

Irradiation of β′-GMO with fast electrons lead to formation of defect centers with luminescent parameters close to those found earlier in many other molybdates and ascribed to oxygen vacancy-related intrinsic defects with formula MoO_3.

Crystal structure was found an important factor influencing luminescence parameters of gadolinium molybdate. Denser crystal structure of α-GMO compared to β′-GMO leads to emission energy shift and the drastic change in temperature dependence of luminescence intensity.

Acknowledgments

The authors express their gratitude to Dr. V.Yu. Ivanov for help in BW3 experiments, Dr. F.G. Neshov for irradiation of samples on M-20 microtron and Prof. V.Ya. Shur for granting crystals. The work was partially supported by HASYLAB (Projects I-20110050, II-20080119 EU), Ural Branch of Russian Academy of Sciences (Project 12-T-3-1003) and Russian Ministry of Education and Science (Grant 14.A18.21.0076).

References

Bacci, M., Mihykova, E., Schulman, L.S., 2002. Quantum corrections to the semi-classical temperature scale in the structured emission of tetrahedral complexes. Physical Review B 66, 132301.

Blasse, G., 1980. The luminescence of closed-shell transition-metal complexes. New developments. Luminescence and Energy Transfer, 1–41.

Blasse, G., Grabmaier, B.C., 1994. Luminescence Materials.

Guo, C., Chen, T., Luan, L., Zhang, W., Huang, D., 2008. Luminescent properties of $R_2(MoO_4)_3$:Eu^{3+} (R=La, Y, Gd) phosphors prepared by sol-gel process. Journal of Physics and Chemistry of Solids 69, 1905–1911.

Guo, X., Zhang, Q., Liu, T., Song, M., Yin, J., Zhang, H., Wang, X.e, 2009. First-principles study on electronic structures of BaMoO4 crystals containing F and F^+ color centers. Nuclear Instruments and Methods in Physics Research Section B: Beam Interactions with Materials and Atoms 267, 1093–1096.

He, X., Zhou, J., Lian, N., Sun, J., Guan, M., 2010. Sm^{3+}-activated gadolinium molybdate: an intense red-emitting phosphor for solid-state lighting based on InGaN LEDs. Journal of Luminescence 130, 743–747.

Itoh, M., 2012. Luminescence study of self-trapped excitons in $CdMoO_4$. Journal of Luminescence 132, 645–651.

Keller, R.C.A., Blasse, G., Lindholm, T., Leskelä, M., 1988. The luminescence of doped and undoped $BaLn_2(MoO_4)_4$ (Ln = La, Gd). Materials Chemistry and Physics 20, 589–598.

Keskar, M., Dahale, N.D., Krishnan, K., Kulkarni, N.K., 2009. Thermal expansion studies of $Gd_2Mo_3O_{12}$ and $Gd_2W_3O_{12}$. Materials Research Bulletin 44, 901–905.

Mikhailik, V.B., Kraus, H., Wahl, D., Mykhaylyk, M.S., 2005. Studies of electronic excitations in $MgMoO_4$, $CaMoO_4$ and $CdMoO_4$ crystals using VUV synchrotron radiation. Physica Status Solidi (b) 242, R17–R19.

Momma, K., Izumi, F., 2011. VESTA 3 for three-dimensional visualization of crystal, volumetric and morphology data. Journal of Applied Crystallography 44, 1272–1276.

Ouwerkerk, M., Kellendonk, F., Blasse, G., 1982. Some observations on the luminescence of rare-earth molybdates with β'-$Gd_2(MoO4)_3$ structure. Journal of the Chemical Society, Faraday Transactions 2 (78), 603–611.

Pan, Y., Zhang, Q., Zhao, C., Jiang, Z., 2007. Luminescent properties of novel Ho^{3+} and Tm^{3+} doped gadolinium molybdate nanocrystals synthesized by the Pechini method. Solid State Communications, 24–27.

Spassky, D., Ivanov, S., Kitaeva, I., Kolobanov, V., Mikhailin, V., Ivleva, L., Voronina, I., 2005. Optical and luminescent properties of a series of molybdate single crystals of scheelite crystal structure. Physica Status Solidi (c) 2, 65–68.

Zeidler, J.R., Ullman, F.G., 1973. Temperature and polarization dependence of the optical absorption edge of gadolinium molybdate. Physical Review B 8, 3371.

Zhang, Y., Holzwarth, N.A.W., Williams, R.T., 1998. Electronic band structures of the scheelite materials $CaMoO_4$, $CaWO_4$, $PbMoO_4$, and $PbWO_4$. Physical Review B 57, 12738.